14

Phase synchronization between time signals extracted from biological data

© O.E. Dick,[1] A.L. Glazov[2]

[1] Pavlov Institute of Physiology, Russian Academy of Sciences,
St. Petersburg, Russia
[2] Ioffe Institute,
St. Petersburg, Russia
e-mail: e-mail: dickviola@gmail.com, glazov.holo@mail.ioffe.ru

Received March 7, 2023
Revised April 18, 2023
Accepted April 19, 2023

The task is to determine the indices of phase synchronization between biological data extracted from neuronal activity and fluctuations in blood pressure and respiration, based on the calculation of instantaneous frequencies and phases using the synchrosqueezed wavelet analysis. Differences in synchronization indices between the analyzed data in two groups of rats (the control group and the group with experimentally induced colitis) were revealed. Pain exposure was found to be associated with frequency adjustment of the variability of the neuronal activity or the blood pressure, followed by the onset of phase synchronization.

Keywords: wavelet transform, phase synchronization, blood pressure fluctuations, neuronal activity.

DOI: 10.61011/TP.2023.06.56534.40-23

Introduction

Studying the interaction between different dynamical systems leading to the occurrence of synchronization is an important task in time series analysis [1]. These interactions are intensively studied in various fields of physics [2–4] and biology [5,6] and are related to the fact that the definition of transitions from an unsynchronized state to a synchronized state [4,7,8] and synchronization duration can be used to assess the degree of control disturbance in physical or physiological systems [6,9–15]. For example, synchronization of the slow component of the heart rate and fluctuations in vascular tone, studied by synchronous recordings of electrocardiograms and photoplethysmograms, is important for clinical cardiology and determination of the functional state of the autonomic regulation of blood circulation for people with cardiovascular diseases [13,16–19].

Synchronization analysis in different electroencephalogram loci in patients with generalized form of epilepsy makes it possible to identify the site of epilepsy [20]. Evaluation of synchronization between intermittent photostimulation and the brain response in the form of electroencephalograms in order to distinguish between responses in groups of patients with high blood pressure and initial manifestations of moderate cognitive impairment and without such manifestations revealed that the decrease in cognitive functions correlates with a longer duration of phase synchronization and a shift in brain responses into a lower frequency range compared to the excitation frequency [14,15], which suggests that synchronization parameters can serve as neurophysiological markers of cognitive impairment.

The interaction of the cardiovascular and respiratory systems includes the nervous monitoring of both systems [21]. Nerve monitoring can lead to synchronized interactions of the nervous, cardiovascular, and respiratory systems, and pathological conditions can alter these interactions. In this regard, determination of the interaction between the variability of arterial blood pressure and the variability of neuronal activity of the brain at the respiratory rate is of particular interest.

The aim of this paper is to evaluate the phase synchronization between the variability of arterial blood pressure and the variability of intervals of neuronal activity of neurons of the reticular formation of the brain at the respiratory rate before and during pain exposure in a group of healthy rats and rats with experimentally induced colitis.

Experiments of this nature in anesthetized animals are being used to study the mechanisms of pain associated with irritable bowel syndrome in humans. Colorectal distension is accompanied in anesthetized rats by brain neuron responses, abdominal muscle contractions, and changes in heart rate and blood pressure [22,23]. Accounting for system responses to pain just expects determination of the interaction between the variability of blood pressure and the variability of neuronal activity of the brain at the respiratory rate during pain exposure.

To assess the phase synchronization between the variability of neuronal activity intervals and the variability of blood pressure intervals at the respiratory rate, the method of synchronously compressed wavelet transformation [24] was

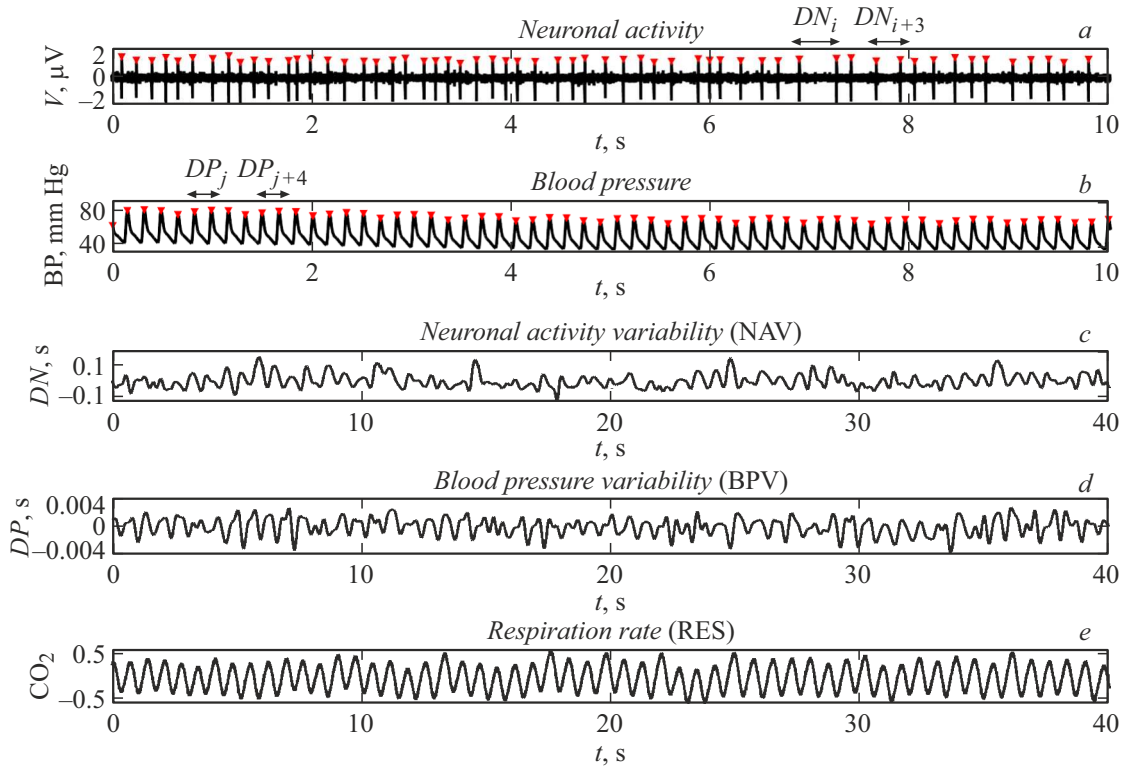

Figure 1. *a* — fragments of neuronal activity, *b* — blood pressure fluctuations, *c* — neuronal activity variability (NAV) curve, *d* — blood pressure variability (BPV) curve, *e* — respiratory rate fluctuations. The intervals DNi and DPi are denoted in *a* and *b*.

used, which allows one to effectively extract instantaneous frequencies and phases from experimental data.

1. Methods

1.1. Experimental data

The analyzed data contained fluctuations in blood pressure, respiration, and neuronal activity in urethane (1.5 mg/kg) anesthetized rats. The data were recorded in the laboratory of cortico-visceral physiology of the Pavlov Institute of Physiology, Russian Academy of Science in accordance with the ethical principles of the International Association for the Study of Pain and the Directive of the Council of the European Community (86/609/EEC). The used data included records before and during painful stimulation of the control group (10 rats) and group (10 rats) with experimental colitis caused by transrectal administration of an alcoholic solution of picrylsulfonic acid (20 mg in 0.2 ml 50% ethanol; TNBS, Sigma, USA) into the colorectal region.

Blood pressure was determined using a pressure sensor located in a catheter placed in the femoral artery (MLT0670, ADInstruments Ltd., UK). Respiratory fluctuations were defined as concentration fluctuations CO_2 measured during inhalation and exhalation using a sensor located in the endotracheal tube (CapnoScan End-Tidal CO2 Monitoring Modular System, USA). Neuronal activity was recorded using a tungsten electrode (WPI, USA) immersed in the brain tissue in the region of the reticular formation of the medulla oblongata.

Mechanical distension of the colorectal region of the large intestine with a rubber balloon inserted rectally was used as pain stimulation. The stimulation duration was 60 s, sampling rate was 10 000 Hz. After 60 s of relaxation, the records were repeated (before and during stimulation) 6 times. For this reason, repeated data were analyzed before and during stimulation.

Fig. 1 shows short fragments (lasting 10 s) of experimental records of neuronal activity and blood pressure fluctuations for a healthy rat (Fig. 1, *a, b*), as well as selected curves of interval variability (DN) of neuronal activity (Fig. 1, *c*), interval variability (DP) of systolic blood pressure (Fig. 1, *d*) and respiration fluctuations (Fig. 1, *e*).

After finding the local maxima, the time intervals between them were determined. Due to the irregularity of the intervals DN and DP, these sequences of intervals are not equidistant. To transform them into equidistant sequences we used approximation by cubic spline and resampling to a frequency of 1000 Hz, and then applied non-linear trend removal. The resulting equidistant sequence of intervals $DN = DN^* - DN_0$ determined the variability of intervals of neuronal activity (NAV), where DN^* — interval without detrending, DN_0 — the magnitude of the trend. Similarly, the equidistant sequence of intervals $DP = DP^* - DP_0$ of blood pressure was found and the curve of blood pressure variability (BPV) was also created without a trend. The

analyzed respiratory oscillations sequences (RES), as well as NAV and BPV, contained at least 60 000 points.

To isolate the components of blood pressure variability and neuronal activity variability with main frequencies close to the respiratory rate, we applied bandpass filtering of the BPV and NAV time series, which removes low-frequency oscillations (< 1 Hz).

1.2. Phase synchronization estimate

The phase synchronization estimation algorithm based on the synchronously compressed wavelet transformation [24] consists of the following sequence of procedures.

1) Making the projection of the wavelet spectrum $(b, f, |W_s(f, b)|^2)$ of the analyzed time series $s(t)$ onto the plane (b, f), where

$$W_s(f, b) = f \int_{-\infty}^{+\infty} s(t)\overline{\psi(f(t-b))}dt, \tag{1}$$

f and b — frequency and time shift, symbol $\bar{\psi}$ means complex conjunction, $\psi(f(t-b))$ — wavelet function obtained from the parent wavelet Gabor-Morlet $\psi(t)$ by scaling and time shift [25]:

$$\psi(f(t-b)) = f\exp(i\omega_0 f(t-b))\exp(-0.5f^2(t-b)^2). \tag{2}$$

2) Making the projection of the synchronously-compressed wavelet spectrum $(b, f, |T_s(f, b)|^2)$ of the analyzed time series $s(t)$ onto the plane (b, f), where

$$T_s(f, b) = \frac{1}{\Delta\omega}\sum_{f_k} W_s(f_k, b) f^{3/2}\Delta f_k,$$

$$f_k:\ |\omega(f_k, b) - \omega_l| \le \Delta\omega/2, \tag{3}$$

circular frequency is determined by the formula

$$\omega_l = (l/n)F_s,\ \ l = 1, \ldots, n,\ \ \Delta\omega = \omega_l - \omega_{l-1} = F_S/n, \tag{4}$$

F_S — sampling frequency of the time series $s(t)$, n — number of scales used when making the wavelet spectrum, $\omega_l - l^{\text{th}}$ discrete circular frequency, $\Delta f_k = f_k - f_{k-1}$.

3) Finding the frequency components of the time series (ridges) by solving the problem of conditional search optimization among all curves that maximize the coefficients of the synchronously compressed wavelet transformation [26]:

$$\omega_r(b) = \arg\max |T_s(\omega_L, b)|,$$

$$\omega_l \in [\omega_r(b) - \Delta\omega/2,\ \ \omega_r(b) + \Delta\omega/2]. \tag{5}$$

4) Finding instantaneous phases and frequencies based on calculated ridges $\omega_r(b)$ according to formulas [26]:

$$f_s(b) = \omega_r(b)/2\pi,\ \ \phi_s(b) = \arg|T_s(\omega_r(b), b)|. \tag{6}$$

5) Further, after finding the instantaneous phases and frequencies for the two analyzed time series, the ratio of instantaneous frequencies $f_s(b)/f_p(b)$ and the instantaneous phase difference are calculated

$$\Delta\phi_{n,m}(b) = (b\phi_s(b) - m\phi_p(b))/2\pi, \tag{7}$$

where n and m — are integers.

6) Phase synchronization of order $n:m$ between two time series is determined by the conditions [5]:

$$|\Delta\phi_{n,m}(b) - c_1| < \varepsilon_1, \tag{8}$$

$$|f_{s1}(b)/f_{s2}(b) - m/n| < \varepsilon_2, \tag{9}$$

where c_1 is a constant and $\varepsilon_1 = 0.03$ and $\varepsilon_2 = 0.03$. This means that during synchronization of phases of order of $n:m$, the instantaneous phase difference oscillates around the constant value c_1, and the value of the ratio of instantaneous frequencies changes around the value m/n.

The time-averaged energy distribution of the synchronously compressed wavelet spectrum by frequencies is determined by the formula [24]:

$$E_{SW}(f) = \int_{t_1}^{t_2} |T_s(f, b)|^2 db. \tag{10}$$

The duration of phase synchronization $n:m$ between two time series is defined as the time interval Δt_{syn} during which the value of the phase synchronization index, calculated according to [27]:

$$\gamma_{n,m} = \left|\left\langle \exp(2\pi i\Delta\phi_{n,m}(b))\right\rangle_{[b+\Delta b]}\right| = \left|\sum_{j=1}^{k}\exp\left(2\pi i\Delta\phi_{n,m}\left(b + \frac{j\Delta b}{k}\right)\right)\right|, \tag{11}$$

close to unity.

Differences between the average values of the duration of phase synchronization for the two groups of data were determined by the method of one-way ANOVA. Statistically significant differences between groups $(k = 2)$ were determined at the significance level of $p < 0.05$, since $n = k(k-1)/2 = 1$ and $1 - 0.95^{1/n} = 0.05$.

2. Results

Fig. 2 shows examples of NAV, BPV, and RES wavelet spectra before (Fig. 2, *a–f*) and during pain exposure (Fig. 2, *g–l*) in the control group rat. The projection of wavelet s[ectra $b, f, |W_s(f, b)|^2$) onto the plane (b, f) obtained as a result of wavelet transformation for the variability of intervals of neuronal activity and the time-averaged distribution of the synchronously compressed wavelet spectrum $|T_s(f, b)|^2$ by frequencies $E_{SW}(f)$ before pain exposure demonstrates the presence of many frequencies in the range from 1 to 3 Hz and the presence of a local

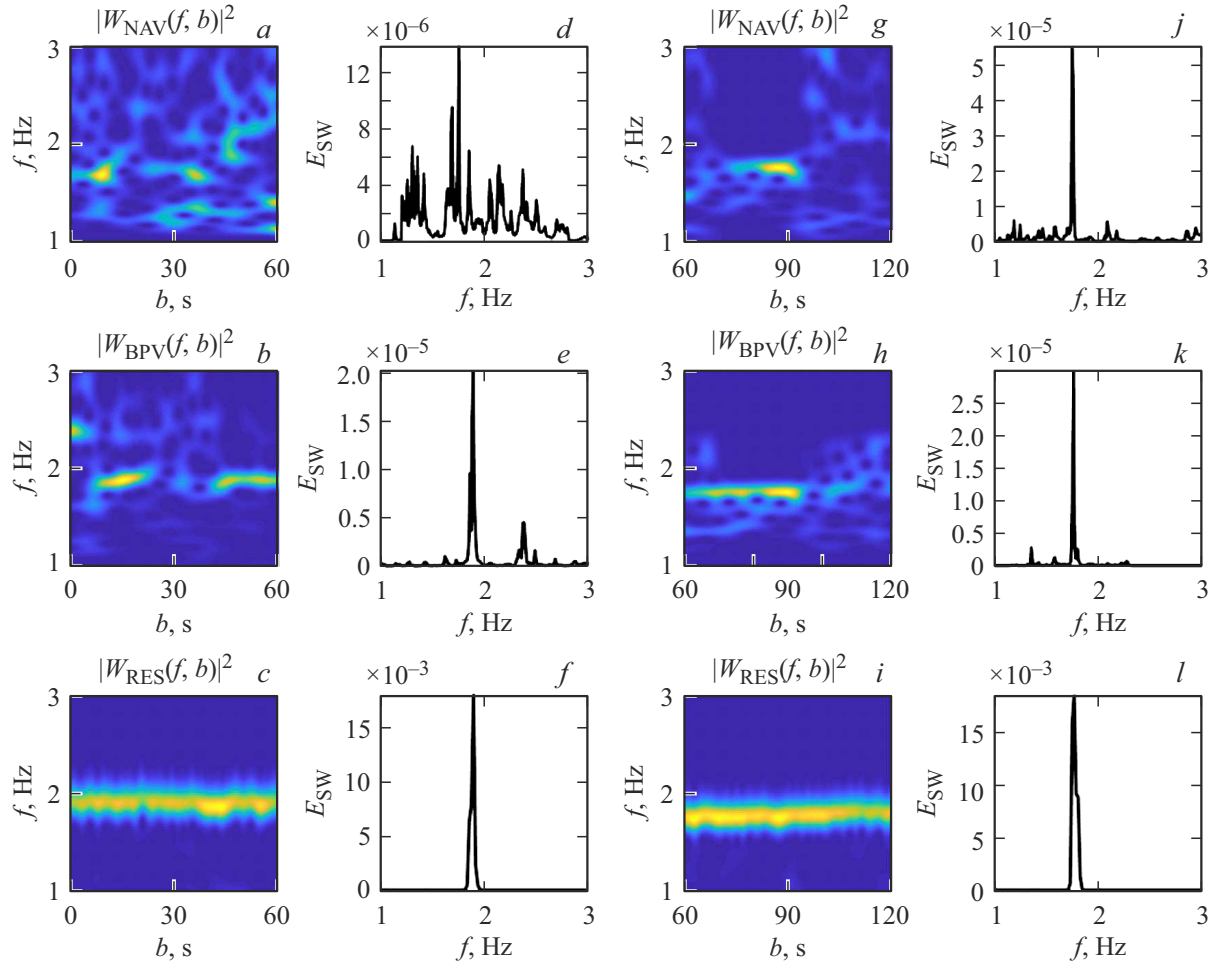

Figure 2. Examples of NAV, BPV and RES wavelet spectra before pain stimulation (a–f) and during stimulation (g–l) healthy rat. a–c and g–i — projections of the wavelet surface $(b, f, |W_s(f, b)|^2)$ onto the plane (b,f) for NAV, BPV and RES; d–f and j–l — time-averaged energy distributions $E_{SW}(f)$ of the synchronously compressed wavelet spectrum $|T_s(f, b)|^2$ by frequencies for NAV, BPV and RES.

maximum near the frequency corresponding to the maxima $E_{SW}(f)$ for respiration and BPV (Fig. 2, d–f).

The time-averaged energy distribution $E_{SW}(f)$ for the variability of blood pressure intervals has maximum at the respiratory rate frequency $f_{RES} = 1.88 \pm 0.03$ Hz (Fig. 2, e,f), but the projection of the wavelet spectrum $(b, f, |W_s(f, b)|^2)$ onto the plane (b, f) shows that this frequency is present in BPV not on the entire time interval (Fig. 2, b).

During pain exposure, the respiratory frequency decreased to the value $f_{RES} = 1.76 \pm 0.03$ Hz, this was accompanied by a decrease in the frequency of blood pressure variability and the appearance of a maximum of neuronal activity variability at the same frequency (Fig. 2, g–l).

Fig. 3 demonstrates the absence of phase synchronization between the rhythms of neuronal activity variability and blood pressure variability before pain exposure in this rat, as well as the presence of phase synchronization between the respiration rhythm and blood pressure variability. The dependence of the ratio of instantaneous frequencies f_{NAV}/f_{BPV} differs from unity (Fig. 3, a), the dependence of the instantaneous phase difference on time $\Delta\phi_{NAV\text{-}BPV}$ has no sections of horizontal plateau (Fig. 3, b), the phase synchronization index $\gamma_{NAV\text{-}BPV}$ fluctuates around a value close to zero (Fig. 3, c). The ratio of instantaneous frequencies f_{BPV}/f_{RES} is close to unity at time intervals 12–26 s and 41–60 s (Fig. 3, d), the instantaneous phase difference $\Delta\phi_{BPV\text{-}RES}$ is close to zero (Fig. 3, e), and the phase synchronization index $\gamma_{BPV\text{-}RES}$ fluctuates around a value close to unity (Fig. 3, f) at these time intervals. This indicates the presence of phase synchronization of the order 1 : 1 and duration $\Delta t_{syn} = \Delta t_{1syn} + \Delta t_{2syn} = 33$ s between the respiration rhythm and blood pressure variability.

Fig. 4 illustrates the presence of phase synchronization between neuronal activity variability and blood pressure variability, as well as between the respiration rate and blood pressure variability during pain stimulation in the same rat. The ratio of instantaneous frequencies f_{BPV}/f_{RES} oscillates around the value close to unity (Fig. 4, a), the instantaneous phase difference $\Delta\phi_{BVP\text{-}RES}$ oscillates around

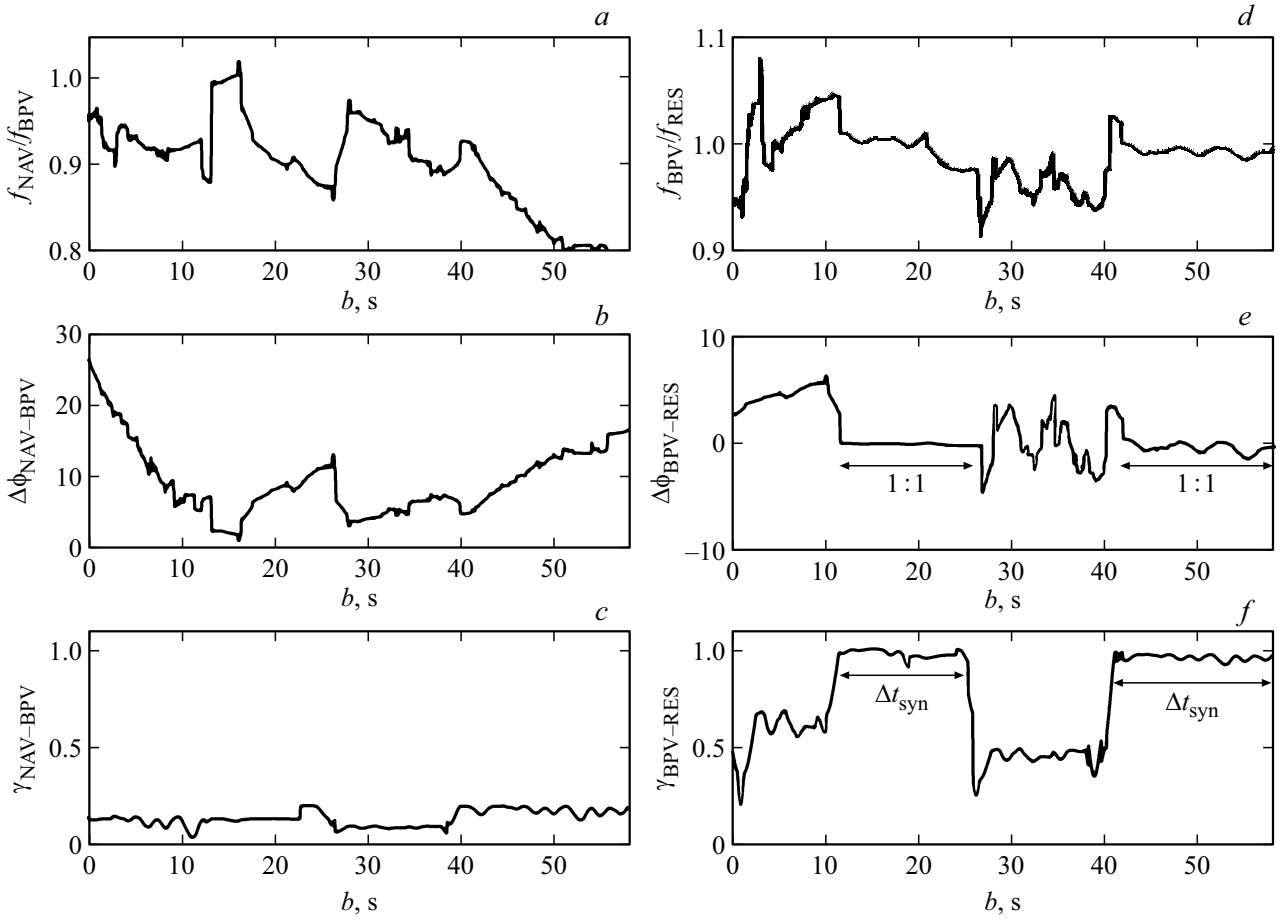

Figure 3. Lack of synchronization between NAV and BPV and presence of synchronization between BPV and RES prior to pain stimulation in the healthy rat. *a, d* — ratios of instantaneous frequencies f_{NAV}/f_{BPV} and f_{BPV}/f_{RES}; *b, e* — instantaneous phase differences $\Delta\phi_{NAV\text{-}BPV}$ and $\Delta\phi_{BPV\text{-}RES}$; *c, f* — dependences of the phase synchronization indices $\gamma_{NAV\text{-}BPV}$ and $\gamma_{BPV\text{-}RES}$ on time.

zero (Fig. 4, *b*), and the phase synchronization index $\gamma_{BPV\text{-}RES}$ oscillates around unity (Fig. 4, *c*) in the time interval 60–93.5 s. The phase synchronization duration in this example is $\Delta t_{syn} = 33.5$ s. At the eighth second from the beginning of exposure, the frequency of neuronal activity variability was adjusted, and synchronization appeared between neuronal activity and blood pressure variability at the respiration rate $f_{RES} = 1.76 \pm 0.03$ Hz. The duration of phase synchronization between NAV and BPV is $\Delta t_{syn} = 29$ s (Fig. 4, *f*). In the time interval 68–97 s, the ratio of instantaneous frequencies f_{NAV}/f_{BVP} fluctuates around a value close to unity (Fig. 4, *d*), the instantaneous phase difference $\Delta\phi_{NAV\text{-}BPV}$ oscillates around zero (Fig. 4, *e*), and the phase synchronization index $\gamma_{NAV\text{-}BPV}$ oscillates around unity (Fig. 4, *f*).

Fig. 5 shows examples of NAV, BPV, and RES wavelet spectra before (Fig. 5, *a–f*) and during pain exposure (Fig. 5, *g–l*) in the rat with experimental colitis. This example is characterized by significant variability in blood pressure intervals and the presence of a local maximum near the frequency $f = 1.52 \pm 0.03$ Hz, corresponding to maxima $E_{SW}(f)$ for respiration and NAV (Fig. 5, *d–f*). During pain exposure there is change in blood pressure variability, and the maximum $E_{SW}(f)$ for BPV at the frequency $f = 1.52$ Hz now corresponds to the maxima $E_{SW}(f)$ for the respiration rate and variability of neuronal activity (Fig. 5, *j–l*).

Fig. 6 illustrates the absence of phase synchronization between BPV and RES, and the presence of phase synchronization between NAV and RES before pain stimulation in the rat, for which wavelet spectra are presented in Fig. 5. The limit of fluctuations of the time dependence of the ratio of instantaneous frequencies f_{BPV}/f_{RES} exceeds the values determined by formula (9) for possible frequency synchronization (Fig. 6, *d*), sections of the horizontal plateau in dependence of instantaneous phase difference on time $\Delta\phi_{BPV\text{-}RES}$ are absent (Fig. 6, *e*), the phase synchronization index $\gamma_{BPV\text{-}RES}$ fluctuates around value close to zero (Fig. 6, *f*). In contrast, on two time intervals 0–38 s and 43–60 s the ratio of instantaneous frequencies f_{NAV}/f_{RES} is close to unity (Fig. 6, *a*), the instantaneous phase difference is close to zero (Fig. 6, *b*), and the phase synchronization index $\gamma_{NAV\text{-}RES}$ fluctuates around value close to unity (Fig. 6, *c*). The duration of synchronization between the

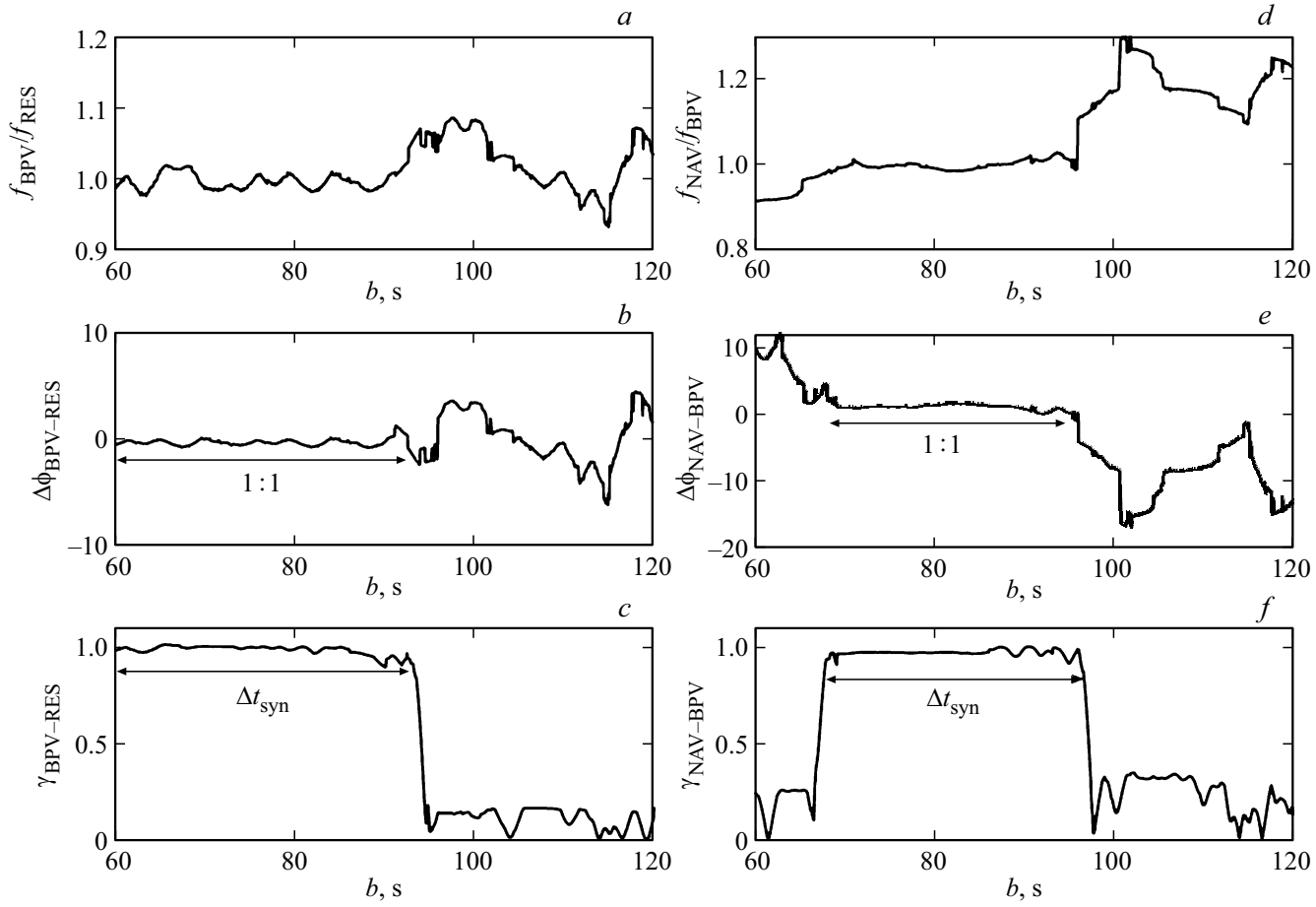

Figure 4. The presence of synchronization between NAV and BPV and between BPV and RES during pain stimulation in healthy rats. *a,f* — are similar to Fig. 3.

respiration rhythm and the variability of neuronal activity is $\Delta t_{syn} = \Delta t_{1syn} + \Delta t_{2syn} = 55$ s.

Fig. 7 demonstrates the synchronization between the respiration rate and blood pressure variability that occurs at the sixth second from the onset of colorectal distension , when the BVP frequency adjusts to the respiratory rate $f_{RES} = 1.54 \pm 0.02$. Synchronization is maintained until the end of the pain exposure, the synchronization duration is $\Delta t_{syn} = 54$ s (Fig. 7,*f*). At the beginning of pain exposure the phase synchronization between the respiration rhythm and the variability of neuronal activity is disturbed, and then restored at the twenty-first second after the onset of exposure and is maintained until the one hundred and sixteenth second. The value of the phase synchronization index $\gamma_{NAV\text{-}RES}$ fluctuates near unity in the time interval [81−116] s (Fig. 7, *c*). The duration of phase synchronization is $\Delta t_{syn\,NAV\text{-}RES} = 35$ s.

Table 1 presents data showing synchronization options before and during pain exposure in two groups of rats. Most of the data (79% of the control group) (subgroup Ia) and (76% of the group with colitis) (subgroup IIa) showed synchronization between blood pressure variability and respiration rate. For 21% of the data of the control group (subgroup Ib) and 24% of the data of the group with colitis (subgroup IIb), synchronization between the respiration rhythm and the variability of neuronal activity was revealed.

For subgroups Ia and IIa, during colorectal distension, synchronization between blood pressure variability and respiration rate is maintained, and synchronization occurs between neuronal activity variability and blood pressure variability.

For subgroups Ib and IIb during pain exposure synchronization is maintained between the respiration rhythm and variability of neuronal activity, and synchronization occurs between the respiration rhythm and blood pressure variability.

Table 2 shows averaged values of phase synchronization durations $\Delta t_{syn\,BPV\text{-}RES}$, $\Delta t_{syn\,NAV\text{-}BPV}$, $\Delta t_{syn\,NAV\text{-}RES}$. During pain exposure, the duration of synchronization between blood pressure variability and respiration rhythm and between neuronal activity variability and blood pressure variability, as well as between neuronal activity variability and respiration rhythm for the group with experimental colitis is less than for the control group ($\Delta t_{syn\,NAV\text{-}RES} = 38 \pm 3$ for subgroup Ib and $\Delta t_{syn\,NAV\text{-}RES} = 34 \pm 3$ for sub-

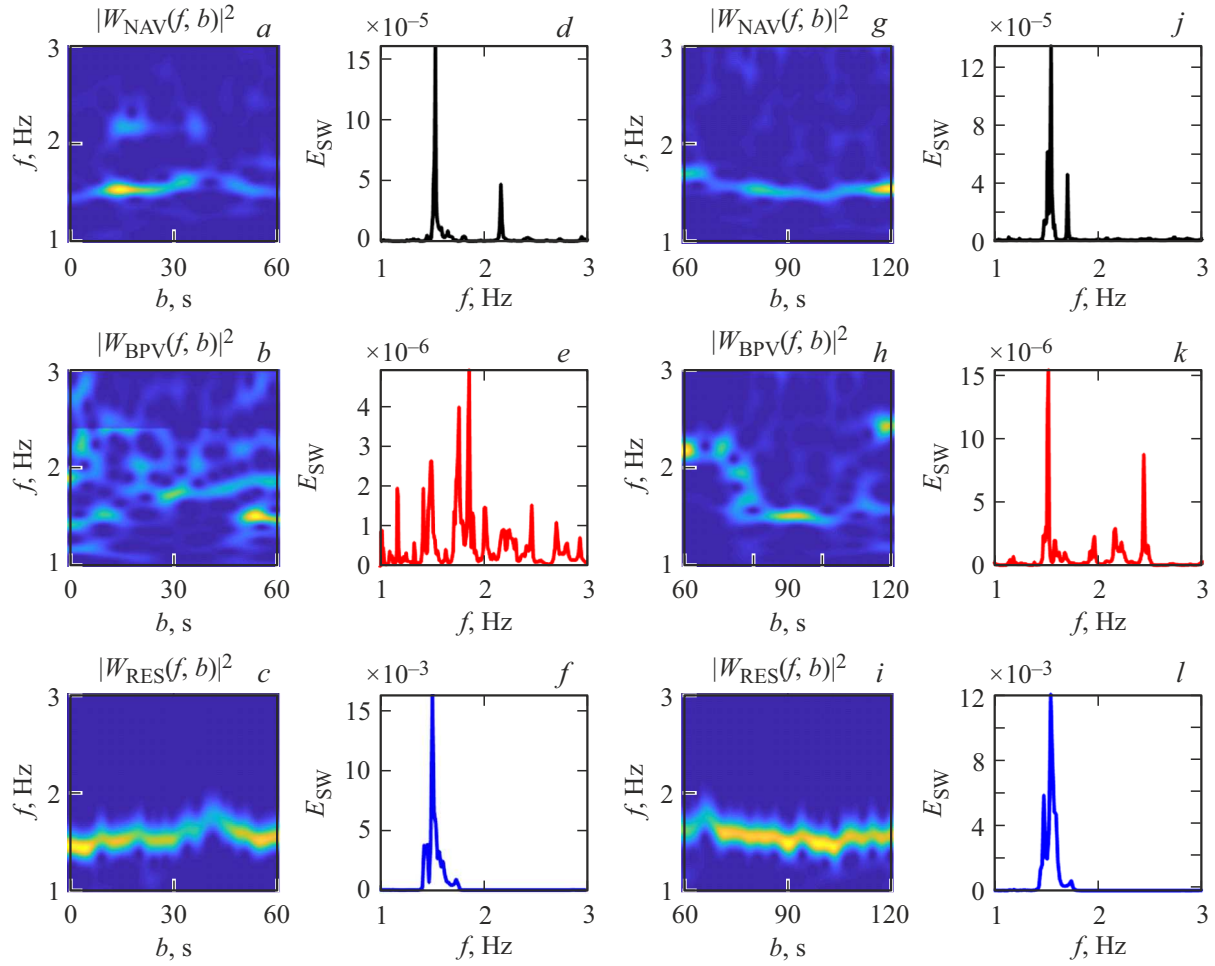

Figure 5. Examples of NAV, BPV and RES wavelet spectra before pain stimulation (a–f) and during stimulation (g–l) rats from the group with colitis. a–l — are similar to Fig. 2.

Table 1. Synchronization options before and during pain exposure

Options	Control group		Group with colitis	
	79% (subgroup Ia)	21% (subgroup Ib)	76% (subgroup IIa)	24% (subgroup IIb)
Before	BVP-RES	NAV-RES	BVP-RES	NAV-RES
During	BVP-RES, NAV-BVP	NAV-RES, BVP-RES	BVP-RES, NAV-BVP	NAV-RES, BVP-RES

group IIb, $\Delta t_{\text{syn NAV-BPV}} = 34 \pm 3$ for subgroup Ib and $\Delta t_{\text{syn NAV-BPV}} = 31 \pm 3$ for subgroup IIb).

For subgroups Ia and IIa the pain exposure increases the duration of phase synchronization between blood pressure variability and respiration rate ($\Delta t_{\text{syn BPV-RES}} = 32 \pm 4$ and $\Delta t_{\text{syn BPV-RES}} = 37 \pm 4$ for subgroup Ia before and during pain exposure, respectively). For subgroups Ib and IIb the pain exposure reduces the duration of phase synchronization between the variability of neuronal activity and the respiration rhythm ($\Delta t_{\text{syn NAV-RES}} = 43 \pm 4$ and $\Delta t_{\text{syn NAV-RES}} = 38 \pm 3$ for subgroup Ib before and during pain exposure, respectively).

Statistically significant differences in mean synchronization durations $\Delta t_{\text{syn BPV-RES}}$, $\Delta t_{\text{syn NAV-BPV}}$, and $\Delta t_{\text{syn NAV-RES}}$ between subgroups Ia and IIa, as well as between subgroups Ib and IIb, were determined at the significance level $p < 0.05$.

Thus, using the phase synchronization analysis method based on the synchronously compressed wavelet transformation, in most of the data on neuronal activity variability, blood pressure variability and respiration rate obtained for the control group of rats and the group of rats with colitis, we found the presence of phase synchronization between the variability of blood pressure and respiration rate in the

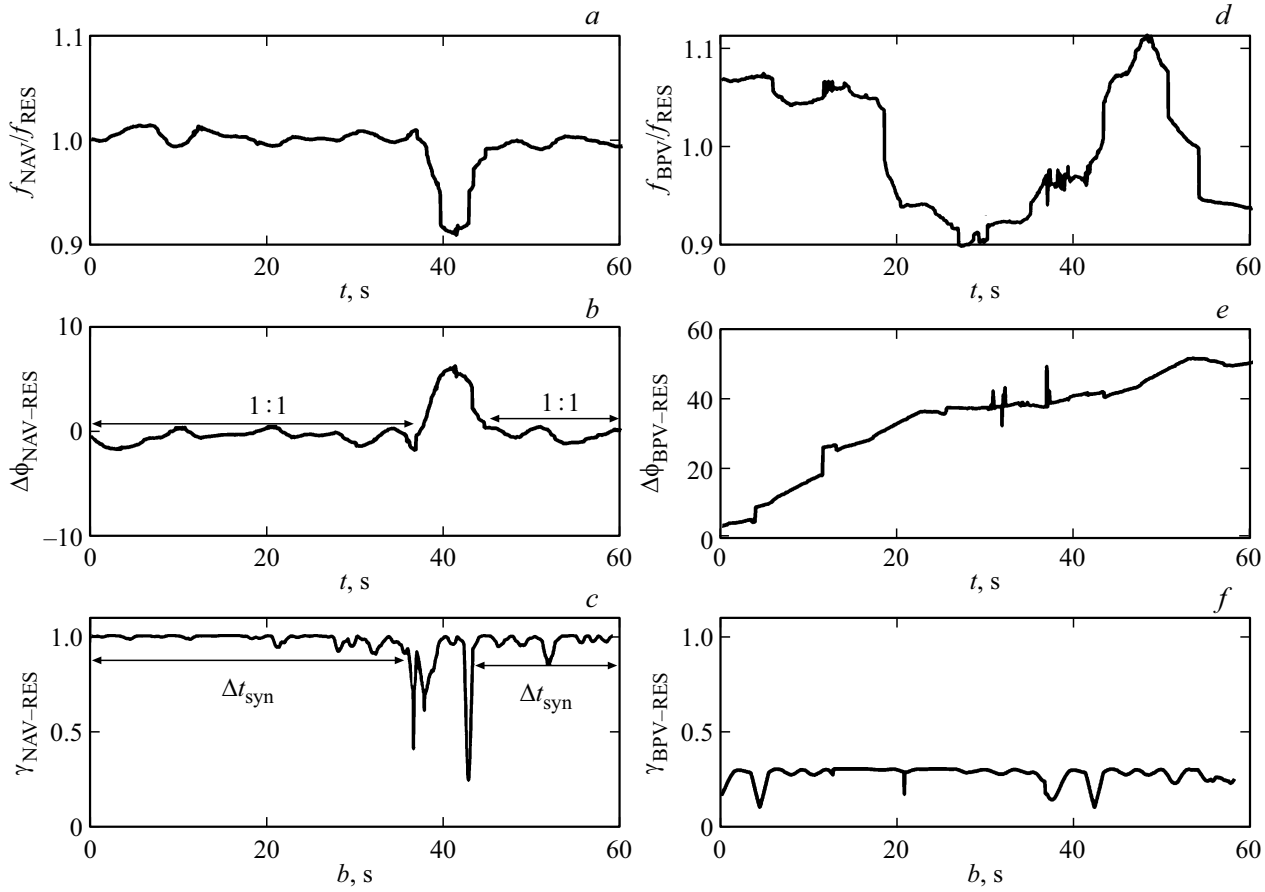

Figure 6. Lack of synchronization between NAV and BPV and presence of synchronization between BPV and RES prior to pain stimulation in the healthy rat. *a, d* — ratios of instantaneous frequencies f_{NAV}/f_{RES} and f_{BPV}/f_{RES}; *b, e* — instantaneous differences of phases and $\Delta\phi_{BPV\text{-}RES}$ *c, f* — dependences of the phase synchronization indices $\gamma_{NAV\text{-}RES}$ and $\gamma_{BPV\text{-}RES}$ on time.

Table 2. Averaged values from phase synchronization durations $\Delta t_{syn\ BPV\text{-}RES}$, $\Delta t_{syn\ NAV\text{-}BPV}$, $\Delta t_{syn\ NAV\text{-}RES}$

Durations Syhchronizations	Control group (subgroup Ia)		Group with colitis (subgroup IIa)	
	Before exposure	During exposure	Before exposure	During exposure
$\Delta t_{syn\ BPV\text{-}RES}$	32 ± 4	37 ± 4	30 ± 3	33 ± 3
$\Delta t_{syn\ NAV\text{-}BPV}$		34 ± 3		31 ± 3
	(subgroup Ia)		(subgroup IIa)	
	BEfore exposure	During exposure	Before exposure	During exposure
$\Delta t_{syn\ BPV\text{-}RES}$		58 ± 6		56 ± 6
$\Delta t_{syn\ NAV\text{-}RES}$	43 ± 4	38 ± 3	53 ± 5	34 ± 3

background data. Painful colorectal distension maintained this synchronization. The frequency of neuronal activity variability adjustment ensured the phase synchronization between neuronal activity and blood pressure variability at the respiration rate some time after onset of the pain exposure beginning Therefore, this work shows for the first time the possibility of detecting synchronization between the variability of arterial blood pressure and the variability of neuronal activity in experimental data for anesthetized rats.

In a smaller number of background data records obtained for the control group of rats and the group of rats with colitis, we revealed the absence of phase synchronization between blood pressure variability and respiration rhythm

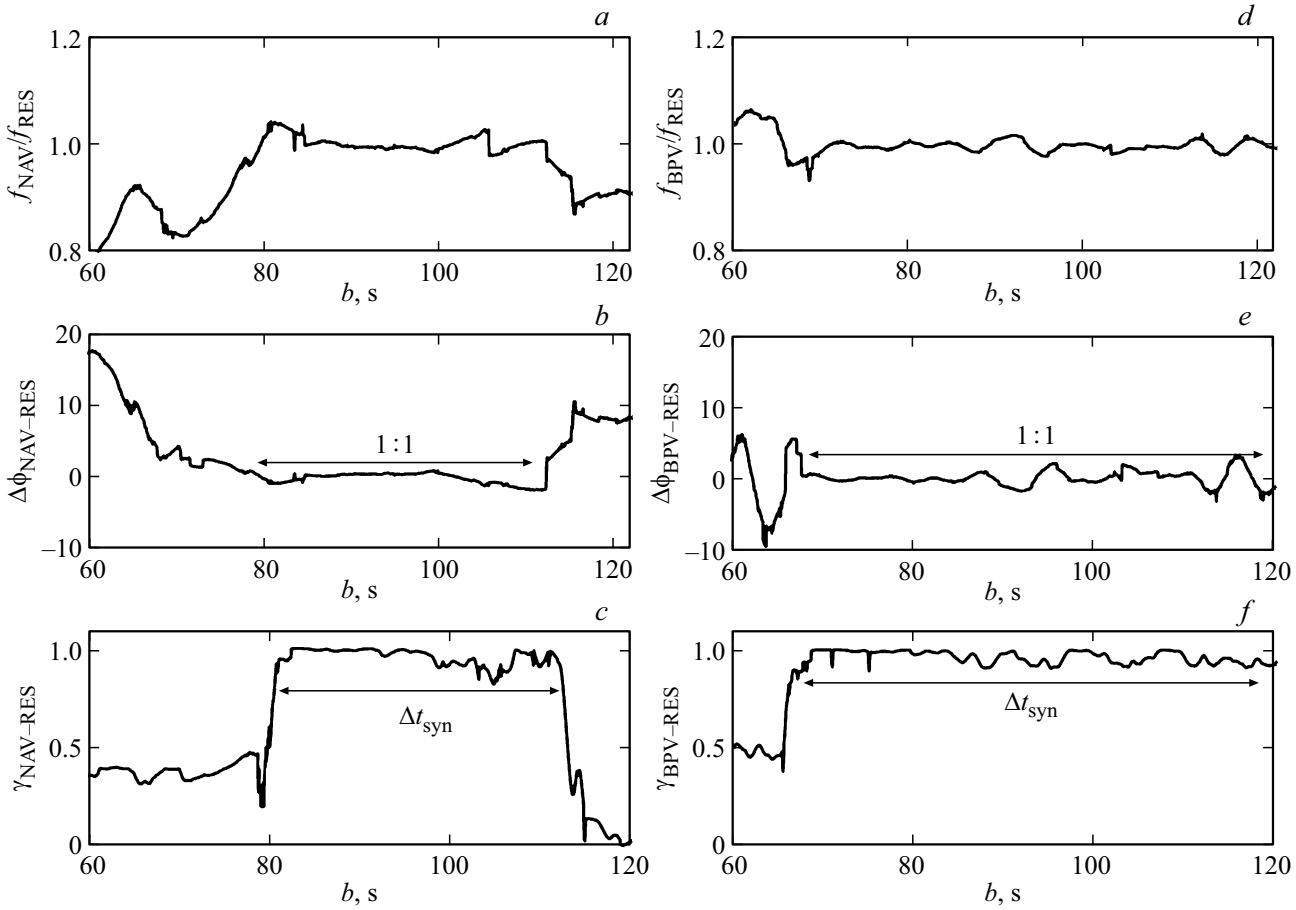

Figure 7. The synchronization between NAV and RES, and between BPV and RES during pain stimulation in group with colitis. *a,f* — are similar to Fig. 6.

and the presence of phase synchronization between neuronal activity variability and respiration rhythm. The pain exposure reduced the duration of phase synchronization by the variability of neuronal activity and the respiration rhythm and caused adjustment of the frequency of arterial pressure variability to the respiration rate, followed by phase synchronization of the arterial pressure variability and the respiration rhythm. This is in agreement with the data that the respiration rhythm, as a rule, controls the rhythm of the cardiovascular system (usually the variability of R−R intervals identified from the electrocardiogram) [5,28–30].

For the group of rats with experimental colitis (compared to the control group) we found the decrease in the duration of phase synchronization between the variability of blood pressure and the respiration rhythm and between the variability of neuronal activity and the variability of blood pressure.

Conclusion

The method of synchronously compressed wavelet transformation made it possible to reveal the possibility of phase synchronization between the variability of neuronal activity and the variability of blood pressure in anesthetized rats and to evaluate the differences in the duration of phase synchronization for different groups of rats (the control group and the group with experimentally induced colitis).

Compliance with ethical standards

All applicable international, national, and/or institutional guidelines for animal care and management were observed.

Acknowledgments

The authors thank O.A Lyubashin, the head of the Lab. of Cortico-Visceral Physiology of Pavlov Institute of Physiology, for providing experimental data.

Conflict of interest

The authors declare that they have no conflict of interest.

References

[1] M. Pikovsky, G. Rosenblum, J. Osipov. Kurths. Physica D, **104**, 219 (1997).

[2] C.M. Ticos, E. Rosa, W.B. Pardo, J.A. Walkenstein, M. Monti. Phys. Rev. Lett., **85**, 2929 (2000).
[3] D.J. DeShazer, R. Breban, E. Ott, R. Roy. Phys. Rev. Lett., **87**, 044101 (2001).
[4] S. Boccaletti, J. Kurths, G.V. Osipov, D. Valladares, C. Zhou. Phys. Reports, **366**, 1 (2002).
[5] A.B. Bespyatov, M.B. Bodrov, V.I. Gridnev, V.I. Ponomarenko, M.D. Prokhorov. Nonlin Phen. Compl. Syst., **6**, 885 (2003).
[6] V.I. Ponomarenko, M.D. Prokhorov, A.B. Bespyatov, M.B. Bodrov, V.I. Gridnev. Chaos, Solitons and Fractals, **23**, 1429 (2005).
[7] I.Z. Kiss, J.L. Hudson. Phys. Rev. E, **64**, 046215 (2001).
[8] S. Boccaletti, E. Allaria, R. Meucci, F.T. Arecchi. Phys. Rev. Lett., **89**, 194101 (2002).
[9] A.E. Hramov, A.A. Koronovskii, V.I. Ponomarenko, M.D. Prokhorov. Phys. Rev. E, **13**, 026208-1 (2006). https://doi.org/10.1103/PhysRevE.73.026208
[10] A.E. Hramov, A.A. Koronovskii, V.I. Ponomarenko, M.D. Prokhorov. Phys. Rev. E, **75**, 056207-1 (2007). DOI: 10.1103/PhysRevE.75.056207
[11] J. Kurths, M.C. Romano, M. Thiel, G.V. Osipov, M.V. Ivanchenko, I.Z. Kiss, J.L. Hudson. Nonlinear Dyn., **44**, 135 (2006). DOI: 10.1007/s11071-006-1957-x
[12] A. Moskalenko, A.A. Koronovskii, A.E. Hramov, M.O. Zhuravlev. JETP Lett., **103** (8), 539 (2016).
[13] A.R. Kiselev, V.I. Gridnev, A.S. Karavaev, et al. Saratovsky nauchno-med. zhurnal, **6**, 328 (2010). (in Russian)
[14] O.E. Dik, A.L. Glazov. Tech. Phys., **66** (4), 661 (2021). DOI: 10.1134/S1063784221040058
[15] O.E. Dick, A.L. Glazov. Neurocomputing, **455**, 163 (2021). https://doi.org/10.1016/j.neucom.2021.05.038
[16] A.R. Kiselev, S.A. Mironov, A.S. Karavaev, D.D. Kulminskiy, V.V. Skazkina, E.I. Borovkova, V.A. Shvartz, V.I. Ponomarenko, M.D. Prokhorov. Physiol Meas, **37** (4), 580 (2016). DOI: 10.1088/0967-3334/37/4/580
[17] E.I. Borovkova, A.S. Karavaev, A.R. Kiselev, V.A. Shvarts, S.A. Mironov, V.I. Ponomarenko, M.D. Prokhorov. Annaly aritmologii, **129**, 136 (2014). (in Russian) DOI: 10.15275/annaritmol.2014.2.7
[18] D. Hoyer, U. Leder, H. Hoyer, B. Pompe, M. Sommer, U. Zwiener. Med. Eng. Phys., **24**, 33 (2002). DOI: 10.1016/S1350-4533(01)00120-5
[19] A.S. Karavaev, M.D. Prokhorov, V.I. Ponomarenko, A.R. Kiselev, V.I. Gridnev, E.I. Ruban, B.P. Bezruchko. CHAOS, **19**, 033112-1 (2009). DOI: 10.1063/1.3187794
[20] D. Rangaprakash, N. Pradhan. Biomed. Signal Proces. Control, **11**, 114 (2014). http://dx.doi.org/10.1016/j.bspc.2014.02.012
[21] Y. Shiogai, A. Stefanovska, P.V.E. McClintock. Phys. Reports, **488**, 51 (2010). DOI: 10.1016/j.physrep.2009.12.003
[22] O.A. Lyubashina, A.A. Mikhalkin, I.B. Sivachenko. Integrative Physiology, **2** (1), 71 (2021). https://www.doi.org/10.33910/2687-1270-2021-2-1-71-78
[23] O.A. Lyubashina, I.B. Sivachenko, A.A. Mikhalkin. Brain Res. Bull., **182**, 12 (2022). DOI: 10.1016/j.brainresbull.2022.02.002
[24] J. Daubechies, H.T. Lu, H.T. Wu. Appl. Comput. Harmon. Anal., **30**, 243 (2011).
[25] J. Daubechies. Ten Lectures on Wavelets, Proc. CMBS-NSF Regional Conf. Series in Applied Mathematics, SIAM Publication **61**, (1992) Ed., Philadelphia, Pennsylvania.
[26] G. Thakur, E. Brevdo, N.S. Fuckar, H.-T. Wu. Signal Proc., **93**, 1079 (2013).
[27] F. Mormann, K. Lehnertz, P. David, C.E. Elger. Phys. D, **144**, 358 (2000).
[28] M.G. Rosenblum, L. Cimponeriu, A. Bezerianos, A. Patzak, R. Mrowka. Phys. Rev. E, **65**, 041909-1 (2002). DOI: 10.1103/PhysRevE.65.041909
[29] R. Mrowka, L. Cimponeriu, A. Patzak, M. Rosenblum. Amer. J. Physiol. Regulatory, Integrative Comparative Physiol., **285** (6), R1395 (2003). DOI: 10.1152/ajpregu.00373.2003
[30] A.J. Ocon, M.S. Medow, I. Taneja, J.M. Stewart. Am J. Physiol Heart Circ Physiol., **300**, 527 (2011). DOI: 10.1152/ajpheart.00257.2010

Translated by I.Mazurov